

Optimizing an Optimization-Based MCA using Perceived Motion Incongruence Models

Cleij, D.; Pool, D.M.; Mulder, Max; Bülthoff, Heinrich H.

Publication date

2020

Document Version

Final published version

Citation (APA)

Cleij, D., Pool, D. M., Mulder, M., & Bülthoff, H. H. (2020). *Optimizing an Optimization-Based MCA using Perceived Motion Incongruence Models*. 53-60. Paper presented at Driving Simulation Conference Europe 2020 VR, Antibes, France.

Important note

To cite this publication, please use the final published version (if applicable).
Please check the document version above.

Copyright

Other than for strictly personal use, it is not permitted to download, forward or distribute the text or part of it, without the consent of the author(s) and/or copyright holder(s), unless the work is under an open content license such as Creative Commons.

Takedown policy

Please contact us and provide details if you believe this document breaches copyrights.
We will remove access to the work immediately and investigate your claim.

Optimizing an Optimization-Based MCA using Perceived Motion Incongruence Models

Diane Cleij^{1,2}, Daan M. Pool², Max Mulder² and Heinrich H. Bühlhoff¹

(1) Max Planck Institute for Biological Cybernetics, Motion Perception and Simulation Group, 72076 Tübingen, e-mail : {diane.cleij, heinrich.buelthoff}@tuebingen.mpg.de

(2) Delft University of Technology, Faculty of Aerospace Engineering, Control & Simulation section, 2629 HS Delft, e-mail : {d.m.pool, m.mulder}@tudelft.nl

Abstract - In this paper the potential of Motion Incongruence Rating (MIR) models for the optimization of Motion Cueing Algorithms (MCAs) is investigated. In a human-in-the-loop simulator experiment, two optimization-based MCAs are compared for a roundabout scenario simulated on a medium-stroke hexapod simulator. The first MCA uses standard cueing error weights from reference literature in its cost function, while for the second case these weights were based on a MIR model fitted to previous experiment data. Results show that such models provide a promising cueing error weight estimation method for optimization-based MCAs, but also highlight the limitations of these models due to, for example, their dependency on the richness of the datasets to which they are fitted.

Keywords: Motion cueing algorithms, motion incongruence models, model predictive control, continuous ratings

Introduction

One of the main challenges in vehicle motion simulation is finding the simulator motions, given vehicle motions and simulator limitations, that result in the highest perceived cueing quality. Lately, more and more optimization-based Motion Cueing Algorithms (MCAs) are being developed which use a cost function based on the difference between simulator and vehicle motions to find an optimal simulator input at each time step [Kat18, Kat17, Fan12, Bru17].

Such optimization-based MCAs avoid the often “worst case” parameter tuning that results from using classical, filter-based MCAs [Gra96]. The cost function in an optimization-based MCA, however, *also* contains many parameters that need to be tuned. Currently, as off-line automatic cueing quality assessment is still difficult, this tuning is generally done by experts [Nas12, Dag09, Beg12].

An example of an optimization-based MCA is the algorithm developed at the Max Planck Institute (MPI) for Biological Cybernetics [Dro18, Kat18, Kat17]. This MCA relies on Model Predictive Control (MPC) to optimize the simulator control inputs at each time step and uses of a mathematical model of the simulator and a prediction of the desired vehicle motions over a specified prediction horizon. The optimization uses a cost function that includes the weighted error between the reference motion, i.e., the vehicle motion, and the simulator motion over this horizon.

In the implementation of this optimization-based MCA, the output includes the simulator’s linear acceleration and rotational velocity. Currently, the algorithm uses generic output weights based on the rough absolute value difference between linear acceleration and rotational velocity, i.e., weights on linear acceleration (in m/s^2) that are on average around

ten times smaller than those on rotational velocity (in rad/s), respectively [Kat15]. These output error weights are thus not chosen based on understanding human motion perception, but purely chosen to account for the differences in output error units.

To directly include knowledge of human perception of motion mismatches into MCA optimization, this paper uses a Perceived Motion Incongruence (PMI) model [Cle20] to objectively retrieve a set of perception-based output error weights. This PMI model was fitted to continuous rating (CR) data obtained in two car driving experiments performed by our team [Cle18, Cle19]. As the resulting cueing error weights correspond to the “best fit” to the CR data, it was expected that these optimized and perception-based weights would indeed result in improved MCA quality compared to generic optimization-based MCA weights.

To assess whether the perception-based output error weights indeed result in improved MCA quality, a human-in-the-loop experiment was performed, where both error weight sets were compared during a passive car driving simulation. The experiment has a similar set up as the previous experiments described in [Cle18] and [Cle19], where the participants experienced (as passengers) a simulation of a Roundabout (RA) section in a hexapod motion simulator and used a continuous rating (CR) method to provide a time-varying measure of cueing quality. Additionally, participants were requested to provide one overall rating (OR) of the cueing quality per condition and fill out a questionnaire, to obtain more insight in the factors affecting their ratings.

Motion Cueing Algorithm

Optimization-based MCA

For the experiment explained in this chapter the Model Predictive Control (MPC)-based MCA designed at the Max Planck Institute (MPI) for Biological Cybernetics [Kat18, Kat17] is used. This MCA uses a linearised model of the hexapod simulator to compute the *future* simulator inputs over a chosen prediction horizon for a provided (future) reference motion. An advantage of this type of MCA, compared to classical filter-based approaches, is that the simulator limits are evaluated explicitly at each time step [May01]. This avoids the need for worst case MCA parameter tuning, often resulting in strongly scaled-down motions [Gra96].

The MPC-based MCA considered here optimizes the simulator inputs \mathbf{u}_k – i.e., the platform specific forces and rotational accelerations – for a desired simulator output, linear acceleration and rotational velocity in head frame, over a prediction horizon. This optimization is performed at each simulation time step and only the first optimized input is actually sent to the simulator. The simulator output $\mathbf{y}(\mathbf{x}_k, \mathbf{u}_k)$ for a given input is compared to a reference motion $\hat{\mathbf{y}}_k$ over this prediction horizon. While ideally this reference motion equals the exact vehicle motions that will occur during this prediction horizon, during active driving these future motions are, of course, unknown. Even though the passive driving experiment described in this paper does not require active driving, for application purposes and realism, the reference motion and prediction horizon length were chosen to be representative for online motion cueing. The reference motion is therefore assumed to be equal to the current vehicle motion and kept constant over a prediction horizon of 2 seconds, as also used in [Kat17].

During the optimization a cost (J) is calculated for a certain set of simulator inputs over the prediction horizon with:

$$J = \|\mathbf{x}_N - \hat{\mathbf{x}}_N\|_{W_{x_N}}^2 + \sum_{k=0}^{N-1} \left(\|\mathbf{x}_k - \hat{\mathbf{x}}_k\|_{W_x}^2 + \|\mathbf{u}_k - \hat{\mathbf{u}}_k\|_{W_u}^2 + \|\mathbf{y}(\mathbf{x}_k, \mathbf{u}_k) - \hat{\mathbf{y}}_k\|_{W_y}^2 \right), \quad (1)$$

where k is the discrete time step, N the prediction horizon length, \mathbf{x} the simulator state vector (platform position/orientation and linear/rotational velocity), \mathbf{u} the simulator inputs (platform specific force and rotational acceleration) and \mathbf{y} the simulator outputs (platform specific force and rotational velocity). The variables $\hat{\mathbf{x}}$, $\hat{\mathbf{u}}$ and $\hat{\mathbf{y}}$ indicate the *reference* state, input and output, respectively. The diagonal matrices $W_{x_N} = \text{diag}(\mathbf{w}_{x_N})^2$, $W_x = \text{diag}(\mathbf{w}_x)^2$, $W_u = \text{diag}(\mathbf{w}_u)^2$ and $W_y = \text{diag}(\mathbf{w}_y)^2$ represent the terminal state, state, input and output error weighting matrices, respectively.

The input and terminal state related costs are used for stability and ensure convexity of the optimization problem [Kat17]. Their references ($\hat{\mathbf{u}}$ and $\hat{\mathbf{x}}_N$) are here set to zero. The weights \mathbf{w}_u and \mathbf{w}_{x_N} were tuned for stability of the output and set to 1 and 2.5, respectively. The state-related cost can be used for washout of the simulator motion when setting its reference $\hat{\mathbf{x}}$ to zero over the full prediction horizon. As

only the platform positions need to be washed out here, the position-related weights of \mathbf{w}_x were set to 4 and the velocity related states were set to zero.

Cost function output weights

The output-related cost in (1) influences how well a certain output channel is reproduced by the simulator platform. This can be tuned with the weights for the different motion channels (specific forces and rotational velocities) in \mathbf{w}_y . The reported standard setting for the weights in \mathbf{w}_y [Kat15] is based on the relative magnitude of specific forces (in m/s^2) and rotational velocities (in rad/s) in typical car manoeuvres, which differs by about a factor of ten. This results in the standard weights, here referred to as \mathbf{w}_{y_s} , as listed in Table 1. These standard weights only account for differences in linear acceleration and rotational velocity units. The possible *relative* importance of perceivable errors in different motion channels for the perceived cueing quality is not taken into account.

Table 1: MPC cost function weight settings.

| Tuning | \mathbf{w}_y weights | | | | | |
|--------------------|------------------------|-------|-------|------------|------------|------------|
| | a_x | a_y | a_z | ω_r | ω_p | ω_y |
| \mathbf{w}_{y_s} | 1 | 1 | 1 | 10 | 10 | 10 |
| \mathbf{w}_{y_p} | 0.71 | 3.32 | 6.17 | 17.87 | 0 | 4.93 |

In this paper, we compare an output error weights setting based on perceived motion incongruence measures, i.e., \mathbf{w}_{y_p} , to the standard weights of \mathbf{w}_{y_s} . The weights for \mathbf{w}_{y_p} , were calculated from a Motion Incongruence Rating (MIR) model fit to the data from the two main driving simulator studies described in [Cle20]. The fit MIR model was a static, zero input delay model with linear acceleration and rotational velocity cueing errors as inputs, which is in fact comparable to the output error related part of the cost function described in (1). The weights of the MIR model were estimated by finding the combination of weights that best described the full set of continuous ratings from both experiments. These weights thus provide an estimate of how much the six different cueing errors likely contributed to participants' perceived motion mismatches. For more details on the MIR model and fitting procedure, please refer to [Cle20]. To obtain an equivalent overall scaling of the perception-based weights, all weights in \mathbf{w}_{y_p} were scaled equally to ensure that the sum of the perception-based weights (\mathbf{w}_{y_p}) equals the sum of the standard weights (\mathbf{w}_{y_s}), see Table 1.

The perception-based weights thus give about three times more weight to a_y and about six times more weight to a_z than \mathbf{w}_{y_s} , while the weight for a_x is reduced by about one third. Using \mathbf{w}_{y_p} is thus expected to result in a better following of the lateral and vertical acceleration. For \mathbf{w}_{y_p} also the roll rate weight is almost a factor 2 higher, while the weight for yaw rate is reduced by around 50% compared to the standard weights. Cueing errors in pitch rate are not penalized at all for \mathbf{w}_{y_p} . As the roll and pitch rates are close to zero during car driving, using \mathbf{w}_{y_p} is expected to result in lower simulator roll rates but higher pitch rates due to tilt coordination than when using \mathbf{w}_{y_s} .

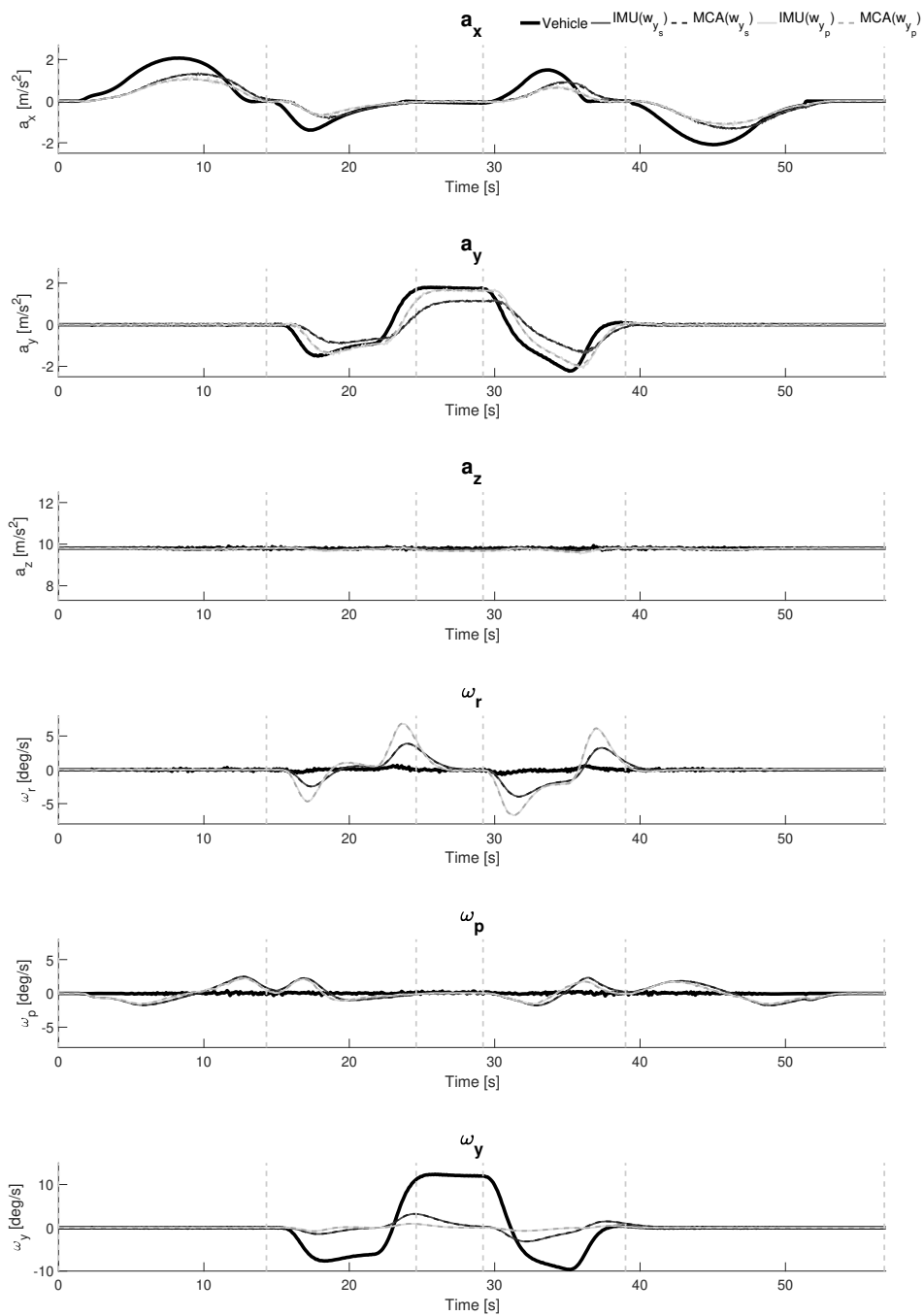


Figure 1: Specific forces and rotational velocities of the car during the car simulation, together with the motions calculated with either w_{y_s} or w_{y_p} and the corresponding measured (IMU) motions on the simulator.

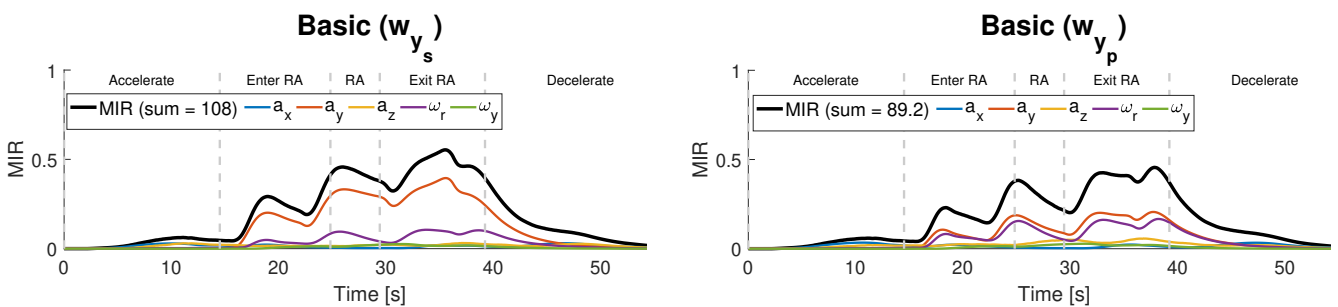


Figure 2: Predicted MIR for simulator motions resulting from either w_{y_s} (left) or w_{y_p} (right).

Predicted cueing quality

To investigate the effects of the different output error weight settings on the simulator motion quality, a short car simulation scenario was defined, including maneuvers with both notable changes in lateral and longitudinal specific force. During the simulation the car first accelerates from standstill to 50 km/h and then slows down to 30 km/h to enter a roundabout. While exiting the roundabout at the second exit, the car accelerates back to 50 km/h and finally decelerates to a full stop. Fig. 1 shows the vehicle specific forces and rotational velocities for this simulation scenario. Additionally, the motions calculated with the MPC-based MCA using either w_{y_s} or w_{y_p} as defined in Table 1 are shown. Finally, Fig. 1 also shows the corresponding motions as measured with the IMU on the simulator platform.

Fig. 1 shows that the different weights mainly affect the amount of tilt coordination that is used to follow the vehicle lateral specific force. When using w_{y_p} the average scaling difference between vehicle and simulator lateral acceleration is around 0.9, while the use of w_{y_s} results in a much lower gain of around 0.6. Additionally, the reduced weight on yaw for w_{y_p} results in a small worsening of the vehicle yaw rate cueing, which is not very good in general due to the use of a hexapod simulator.

To verify if using the optimized perception-based weights w_{y_p} indeed reduces the predicted MIR, the MCA outputs shown in Fig. 1 were fed through the fit MIR model that was also used to estimate w_{y_p} . The resulting predicted MIR as a function of time is shown in Fig. 2 for w_{y_x} (left) and w_{y_p} (right). The sum of the predicted MIR over time for both MCA settings is indicated in the legend of each plot and shows that indeed better motion quality, i.e., an overall lower MIR of around 17%, is predicted for w_{y_p} . The largest differences occur during the roundabout (RA) section and for the MIR caused by a_y cueing errors.

Experiment

For experimental comparison of the differences between using w_{y_s} and w_{y_p} as the error weights for an MPC-based MCA, a human-in-the-loop driving simulator experiment was performed. In the experiment, participants experienced the same driving scenario introduced in the previous section as passengers for both error weight settings. Their subjective impression of the resulting motion quality was measured using the same subjective rating method as in [Cle18].

Independent Variables and Dependent Measures

The only independent variable of the experiment was the output error weight setting of the MPC-based MCA, as listed in Table 1. We compare the baseline (w_{y_s}) weights [Kat15] with those optimized based on previously measured perceived motion incongruence (w_{y_p}) [Cle20].

The dependent measures are the measures for MCA quality, obtained using the Continuous Rating (CR)

method from [Cle18], resulting in a continuous rating of the cueing quality throughout the simulation for each participant. In addition, participants provided a separate overall rating (OR) after each simulation trial, resulting in one quality rating per condition. To be able to verify the consistency of the participants' ratings, both the CR and OR measurements were repeated three times for both MCA settings.

As the MIR model analysis (see Fig. 2) predicts a lower MIR when using the optimized w_{y_p} output error weights instead of the heuristically-tuned weights w_{y_s} , the hypothesis is that the perceived motion cueing quality improves. This improvement should be visible in both the measured OR and CR data, especially throughout the roundabout section.

Apparatus

The experiment was performed in the CyberPod Simulator at the MPI for Biological Cybernetics, which has a hexapod motion platform (eMotion-1500-6DOF-650-MK1 from Bosch Rexroth) with a stroke length of 0.65 m. The experiment set up is shown in Fig. 3. The visuals were projected on a screen about one meter in front of the participant using a VPixx technologies ProPixx beamer with 1920x1080 resolution and a 120 Hz update rate, providing the participants with a 80-deg horizontal field-of-view.

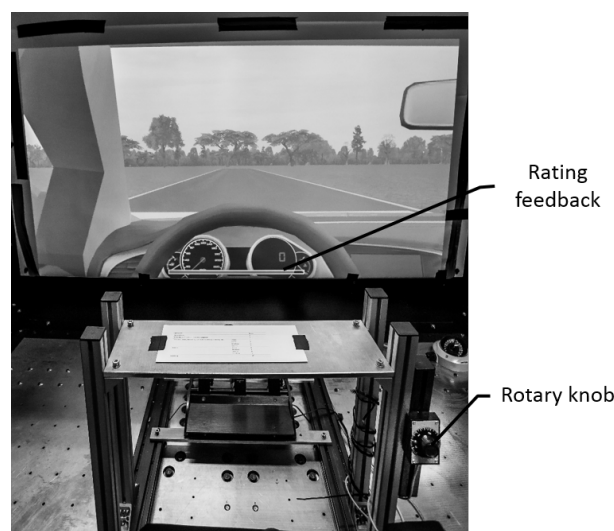


Figure 3: Experiment set up in the hexapod simulator of the MPI for Biological Cybernetics.

The vehicle motions were generated using CarSim software and the visuals were generated using Unity. The steering wheel in the visuals was animated using the steering wheel angle provided by CarSim. The participants used a custom made rotary knob with visual feedback in the form of a rating bar to provide their rating during the experiment, see Fig. 3.

Participants

15 participants, of which five female, performed the experiment. The participants were between 20 and 61 years (average of 30 years) old and all possessed a valid car driving license. All but three participants had no prior knowledge or experience with motion

cueing algorithms. Participants volunteered to perform the experiment and those not working at the MPI were compensated for their time (eight euros per hour).

Instructions and Procedures

The task of the participants was to rate the perceived motion incongruence, or mismatch, between the visual and inertial motions during a passive car driving simulation. After reading the experiment instructions, participants were further briefed about the goal of the experiment and their tasks verbally.

The experiment started with a training phase in which the simulation scenario was experienced twice for both MCA settings, i.e., four simulation trials in total. Throughout the experiment, the simulation trials were performed in pairs including both MCA settings, but the order of the setting within one pair was randomized across participants. During the first repetition of such a trial pair, participants were asked to observe the mismatches and try to anchor the rating scale to the minimum and maximum mismatch perceived over both simulations. During the second repetition, participants were requested to use the anchored rating scale to provide a continuous rating (CR) throughout the simulations, by moving the rating bar on the screen using a rotary knob. After each simulation they were also requested to provide an overall rating (OR) on the same scale, indicating a summary of their continuous rating, using the rotary knob.

After this training phase, another three repetitions per MCA setting, i.e., in total six simulation trials, were performed to collect, as consistently as possible, the CR and OR data for analysis.

To monitor simulator sickness a misery score (MISC) [Bos05] was requested after each simulation pair. The total experiment lasted around 45 minutes per participant and none of the participants became sick.

Data processing and analysis

For each participant the OR and the CR data were collected for three repeated simulation trials of both MCA settings. Each participant was explicitly asked to anchor the rating scale to the maximum and minimum mismatch present during the two simulation and thus use the whole rating scale for their CR for each simulation pair. To correct for any remaining discrepancies, the CR data were normalized in post-processing, such that both the maximum and minimum ratings were obtained at least once during each pair of trials. For each participant, the final OR or CR per MCA setting was calculated as the mean over all three repetitions.

To determine whether significant differences are present between the MCA settings, statistical tests were performed. For comparisons between sufficiently normally distributed data, a two-sample *t*-test was performed and the *t*-statistic, degrees-of-freedom and *p*-value are reported. For those comparisons that include non-normal data, a Wilcoxon signed-ranks test was used instead and the corresponding *W*-statistic, or for bigger samples the *Z*-statistic, and *p*-value are reported.

Results

Rating consistency

During the experiment the participants were asked to judge the perceived motion incongruence by giving both a Continuous Rating (CR) and an Overall Rating (OR) for each MCA setting. Although subjective ratings are likely not to be exactly the same for each repetition, it is expected that participants at least consistently prefer the same MCA. To determine if the participant understood and performed the given task correctly, here the consistency of this preference is checked. All but two of the 15 participants indeed showed a consistent preference for one of the MCAs, i.e., only Participants 1 and 11 changed their preference across the different repetitions and thus did not show a consistent preference. Their OR results are therefore excluded from further analysis.

The consistency of the CR data was also checked for each of the fifteen participants. Following the same approach taken before [Lam11, Cle18, Cle19, Lee19], consistency is calculated with Cronbach's alpha (α) [Cro51]. Sets of ratings with an α below 0.7 are considered inconsistent [Hai10] and are excluded from further CR analysis.

In total, 11/15 participants showed consistent CRs (mean α : 0.89, std: 0.061). Fig. 4 shows example CR data of two participants who are either very inconsistent ($\alpha = 0.58$) or very consistent ($\alpha = 0.96$) across the three trials. With α values of 0.58, 0.53, 0.55 and 0.51, Participants 1, 3, 9 and 12, respectively, gave inconsistent CRs and their results are thus excluded from the CR analysis.

Participant groups

The data showed that not all participants had the same MCA preference. Next to presenting the overall (averaged) rating results, the results of two participant groups, namely those preferring w_{y_s} and those preferring w_{y_p} , will therefore also be shown in this paper. In Fig. 5 the relative rating differences between MCA settings are shown for both the mean OR and CR per participant. The gray colored bars indicate the participants that were excluded from further analysis of either the OR or CR data due to lacking consistency.

Fig. 5 shows that all participants except Participant 1, showed a consistent preference when rating with the OR or CR. Five out of the fourteen participants preferred w_{y_p} , while nine preferred the generic w_{y_s} setting. In the next section, all results are shown separately for these two groups.

Rating results

Overall ratings (OR)

For the analysis of the ORs, the consistent data of 13 participants are used. For each participant one OR per MCA setting is calculated as the average over three repetitions. In Fig. 6 the OR data results for all consistently rating participants, as well as for each participant group – w_{y_s} preferred ($N = 9$) and w_{y_p} preferred ($N = 4$) – are shown in a boxplot.

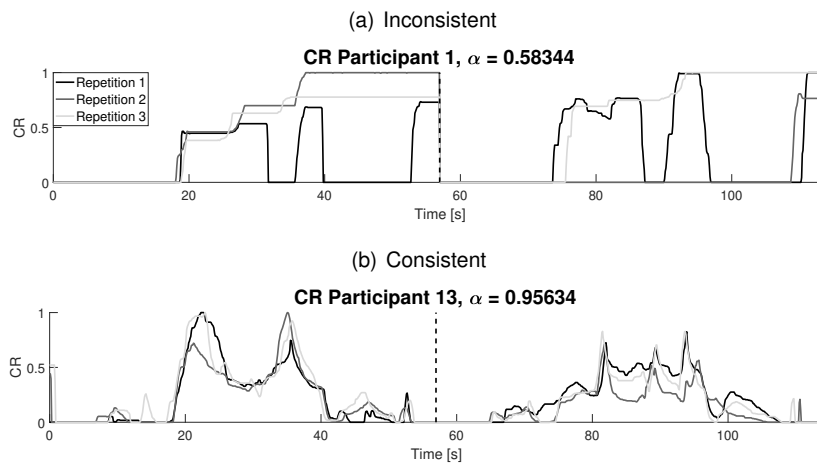


Figure 4: Examples of inconsistent and consistent participant continuous ratings.

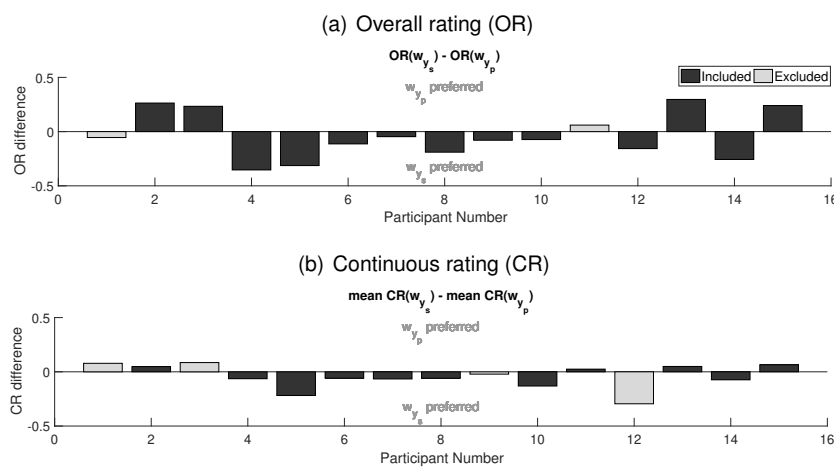


Figure 5: Rating differences between both MCA settings per participant. A positive or negative difference indicates a preference for settings w_{y_p} or w_{y_s} , respectively.

For all participants combined, see Fig. 6, no significant difference between the two MCA settings was found ($t(24) = 0.58, p \geq 0.05$), nor for the participant group that preferred w_{y_s} ($t(16) = 2.09, p \geq 0.05$). For the participants who preferred w_{y_p} the difference in OR between the MCA settings (mean OR for $w_{y_s} = 0.57$, mean OR for $w_{y_p} = 0.31$) was found to be significant ($t(6) = 4.15, p < 0.05$).

Continuous ratings (CR)

For the CR data analysis, the consistent data of 11 participants are used, see Fig. 5. The CR per participant is calculated as the mean over all three repetitions. Fig. 7 shows the median and interquartile range of the CRs across all participants per MCA setting for all consistently rating participants, as well as the two participant groups, i.e., w_{y_s} preferred ($N = 7$) and w_{y_p} preferred ($N = 4$). The figures are divided in five sections, each showing the data belonging to a different section of the simulation, with RA referring to Roundabout.

Fig. 7 shows that the CRs mainly increase during the roundabout section of the simulation scenario for both MCA settings. Especially Fig. 7(a) indicates

that overall the difference between the two MCA settings is relatively small. For a more direct comparison of the CR data between the two MCA settings, the CR of each participant is summarized with the time-averaged mean CR over all time steps. Fig. 8 shows the resulting time-averaged mean CR data in boxplots, matching the presentation of the OR data in Fig. 6.

From Figs. 7 and 8 it is clear that when looking at the CR data for all participants, no significant differences seem to be present. Statistical analysis of the time-averaged mean CR confirms this ($t(20) = 0.8735, p \geq 0.05$). While the CR data show the same effects observed for the OR data for the two participants groups, overall the CR differences for both the participant groups preferring w_{y_s} ($t(12) = 1.5047, p \geq 0.05$) and preferring w_{y_p} ($t(6) = 0.5933, p \geq 0.05$) are not found to be statistically significant.

Conclusions

In this paper an example of how Motion Incongruence Rating (MIR) models [Cle20] can be used for Motion Cueing Algorithm (MCA) optimization is explained and tested. The obtained results do not show

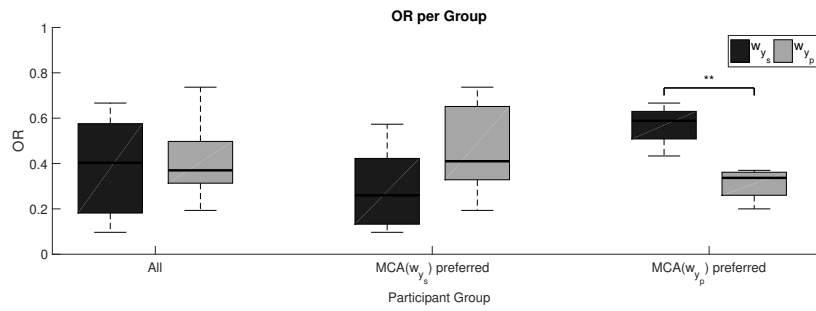


Figure 6: Boxplots of the mean Overall Rating (OR) over three repetitions for participants with a consistent OR. The box shows the interquartile range and the median over all ratings.

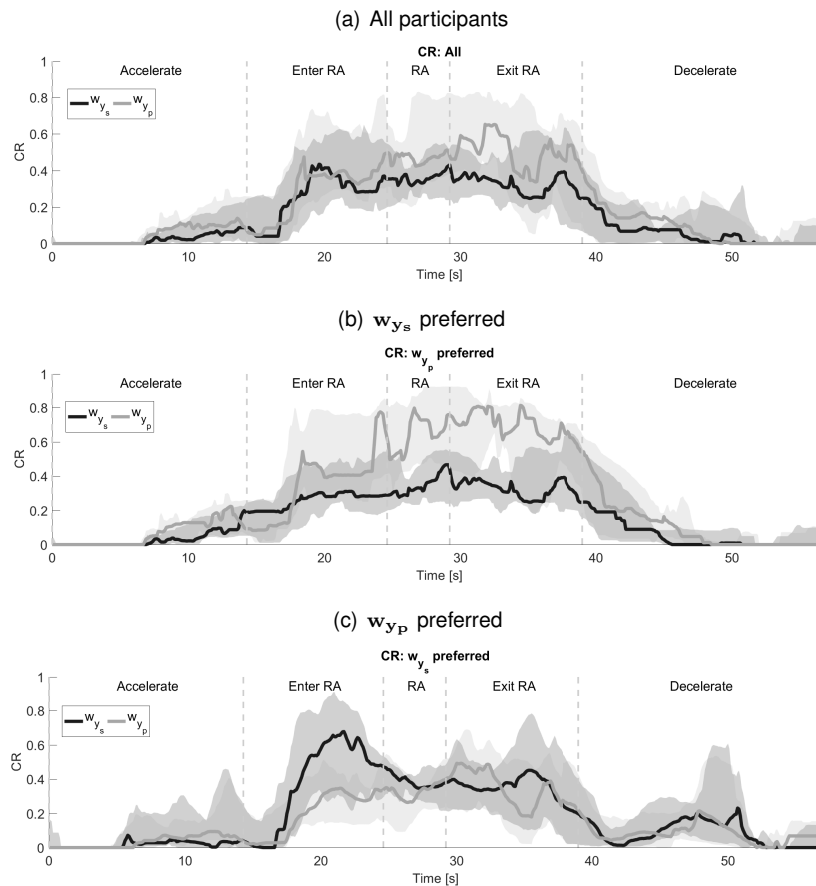


Figure 7: Median CR (solid lines) and interquartile range (shaded) for all participants (a) and those preferring w_{y_s} (b) and w_{y_p} (c), respectively.

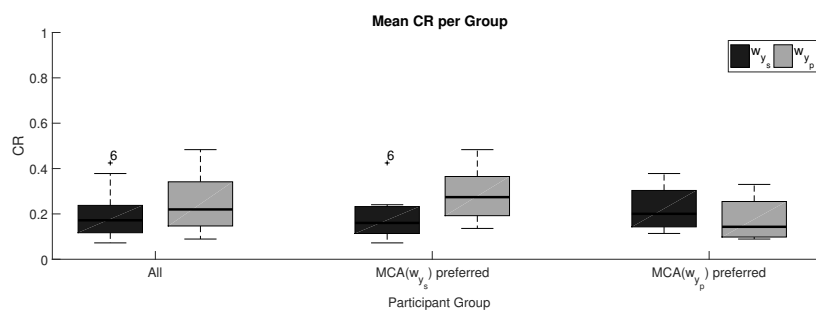


Figure 8: Boxplots of the mean CR over time and all three repetitions per MCA setting for participants with a consistent CR. The box shows the interquartile range and the median over all ratings.

a clear difference between the cueing quality of an optimization-based MCA optimized with the help of a MIR model and a generic tuning based on the typical variance difference between specific forces and rotational velocities for typical car manoeuvres.

Unexpectedly, more participants preferred the generic tuning as compared to the optimization using MIR models. This preference seems to mainly be based on a preference for lower than unity gains between vehicle and simulator motions [Cor14]. The predicted preference for the optimization using MIR models did hold for about one third of the participants. Additionally, the low impact of cueing errors in longitudinal motions as compared to lateral motions was also predicted accurately.

The fact that for one third of the participants optimization using a MIR model was preferred indicates that, while not as broadly applicable as was done here, MIR models can be useful for MCA optimization. It is expected that more sophisticated MIR models (i.e., models that separately account for different cueing error types [Cle20]) estimated from a much richer dataset will result in an MCA that is preferred by a wider range of participants. To fully understand the use of MIR models for MCA optimization, however, it is recommended to first further develop these models under conditions that are more similar to those which the resulting optimized MCA quality will be tested under, such as the same motion platform, visual system and participant group.

References

- A. Beghi, M. Bruschetta and F. Maran, **A real time implementation of MPC based Motion Cueing strategy for driving simulators**, in IEEE Conference on Decision and Control, 6340–6345, IEEE, Maui, Hawaii, USA, 2012.
- J. E. Bos, S. N. MacKinnon and A. Patterson, **Motion sickness symptoms in a ship motion simulator: effects of inside, outside, and no view.**, *Aviation, space, and environmental medicine*, vol. 76(12): 1111–8, 2005.
- M. Bruschetta, F. Maran and A. Beghi, **A nonlinear, MPC-based motion cueing algorithm for a high-performance, nine-DOF dynamic simulator platform**, *IEEE Transactions on Control Systems Technology*, vol. 25(2): 686–694, 2017.
- D. Cleij, J. Venrooij, P. Pretto, D. M. Pool, M. Mulder and H. H. Bülthoff, **Continuous subjective rating of perceived motion incongruence during driving simulation**, *IEEE Transactions on Human-Machine Systems*, vol. 48(1): 17–29, 2018.
- D. Cleij, J. Venrooij, P. Pretto, M. Katliar, H. H. Bülthoff, D. Steffen, F. W. Hoffmeyer and H. P. Schöner, **Comparison between filter- and optimization-based motion cueing algorithms for driving simulation**, *Transportation Research Part F: Traffic Psychology and Behaviour*, vol. 61: 53–68, 2019.
- D. Cleij, **Measuring, Modelling and Minimizing Perceived Motion Incongruence for Vehicle Motion Simulation**, Ph.D. thesis, Delft University of Technology, Faculty of Aerospace Engineering, 2020.
- B. J. Correia Grácio, J. E. Bos, M. M. Van Paassen and M. Mulder, **Perceptual Scaling of Visual and Inertial Cues. Effects of Field of View, Image Size, Depth Cues, and Degree of Freedom**, *Experimental Brain Research*, vol. 232: 637–646, 2014.
- L. J. Cronbach, **Coefficient alpha and the internal structure of tests**, *Psychometrika*, vol. 16(3): 297–334, 1951.
- M. Dagdelen, G. Reymond, A. Kemeny, M. Bordier and N. Maïzi, **Model-based predictive motion cueing strategy for vehicle driving simulators**, *Control Engineering Practice*, vol. 17(9): 995–1003, 2009.
- F. M. Drop, M. Olivari, M. Katliar and H. H. Bülthoff, **Model Predictive Motion Cueing: Online Prediction and Washout Tuning**, in Driving Simulator Conference, 71–78, Antibes, France, 2018.
- Z. Fang and A. Kemeny, **Explicit MPC motion cueing algorithm for real-time driving simulator**, in Power Electronics and Motion Control Conference, 874–878, Harbin, China, 2012.
- P. R. Grant, **The Development of a Tuning Paradigm for Flight Simulator Motion Drive Algorithms**, Phd thesis, University of Toronto, 1996.
- J. F. jr. Hair, W. C. Black, B. J. Babin and R. E. Anderson, **Multivariate Data Analysis**, Pearson Prentice Hall, Upper Saddle River, NJ, USA, 7th ed., 2010.
- M. Katliar, K. N. de Winkel, J. Venrooij, P. Pretto and H. H. Bülthoff, **Impact of MPC Prediction Horizon on Motion Cueing Fidelity**, in Driving Simulation Conference, 219–222, Tübingen, Germany, 2015.
- M. Katliar, J. Fischer, G. Frison, M. Diehl, H. Teufel and H. H. Bülthoff, **Nonlinear Model Predictive Control of a Cable-Robot-Based Motion Simulator**, *IFAC-PapersOnLine*, vol. 50(1): 9833–9839, 2017.
- M. Katliar, F. M. Drop, H. Teufel, M. Diehl and H. H. Bülthoff, **Real-Time Nonlinear Model Predictive Control of a Motion Simulator Based on a 8-DOF Serial Robot**, in European Control Conference, 1529–1535, Limassol, Cyprus, 2018.
- M. Lambooi, W. A. Ijsselsteijn and I. Heynderickx, **Visual discomfort of 3D TV: Assessment methods and modeling**, *Displays*, vol. 32(4): 209–218, 2011.
- T. D. van Leeuwen, D. Cleij, D. M. Pool, M. Mulder and H. H. Bülthoff, **Time-varying perceived motion mismatch due to motion scaling in curve driving simulation**, *Transportation Research Part F: Traffic Psychology and Behaviour*, vol. 61: 84–92, 2019.
- D. Mayne, **Control of Constrained Dynamic Systems**, *European Journal of Control*, vol. 7(2-3): 87–99, 2001.
- A. R. Naseri and P. R. Grant, **An Improved Adaptive Motion Drive Algorithm**, in AIAA Modeling and Simulation Technologies Conference, 1–9, San Francisco, CA, USA, 2012.